Semi-automatic Cardiac and Respiratory Gated MRI for Cardiac Assessment During Exercise

Bram Ruijsink[1,2(✉)], Esther Puyol-Antón[1], Muhammad Usman[1,3], Joshua van Amerom[1], Phuoc Duong[1,2], Mari Nieves Velasco Forte[1,2], Kuberan Pushparajah[1,2], Alessandra Frigiola[1,2], David A. Nordsletten[1], Andrew P. King[1], and Reza Razavi[1,2]

[1] Division of Imaging Sciences and Biomedical Engineering, King's College London, London, UK
jacobus.ruijsink@kcl.ac.uk
[2] Guy's and St Thomas' Hospital NHS Foundation Trust, London, UK
[3] Department of Computer Science, University College London, London, UK

Abstract. Imaging of the heart during exercise can improve detection and treatment of heart diseases but is challenging using current clinically applied cardiac MRI (cMRI) techniques. Real-time (RT) imaging strategies have recently been proposed for exercise cMRI, but respiratory motion and unreliable cardiac gating introduce significant errors in quantification of cardiac function. Self-navigated cMRI sequences are currently not routinely available in a clinical environment. We aim to establish a method for cardiac and respiratory gated cine exercise cMRI that can be applied in a clinical cMRI setting. We developed a retrospective, image-based cardiac and respiratory gating and reconstruction framework based on widely available highly accelerated dynamic imaging. From the acquired dynamic images, respiratory motion was estimated using manifold learning. Cardiac periodicity was obtained by identifying local maxima in the temporal frequency spectrum of the spatial means of the images. We then binned the dynamic images in respiratory and cardiac phases and subsequently registered and averaged them to reconstruct a respiratory and cardiac gated cine stack. We evaluated our method in healthy volunteers and patients with heart diseases and demonstrate good agreement with existing RT acquisitions ($R = .82$). We show that our reconstruction pipeline yields better image quality and has lower inter- and intra-observer variability compared to RT imaging. Subsequently, we demonstrate that our method is able to detect a pathological response to exercise in patients with heart diseases, illustrating its potential benefit in cardiac diagnostic and prognostic assessment.

Keywords: Exercise MRI · Cardiac imaging · Image-based motion correction · Manifold learning

1 Introduction

Assessment of cardiac volumes, function and wall motion using cardiac Magnetic Resonance Imaging (cMRI) during physiological stress (exercise) has a

M.J. Cardoso et al. (Eds.): CMMI/RAMBO/SWITCH 2017, LNCS 10555, pp. 86–95, 2017.
DOI: 10.1007/978-3-319-67564-0_9

great potential to improve early diagnosis, treatment evaluation and prognostic stratification in patients with heart disease [2,10]. Unfortunately, visualising the heart during exercise is challenging using routine clinical cMRI as bodily movements and the inability to breath hold severely corrupt quality of the images (see Fig. 3a).

In an attempt to enable imaging during exercise, several clinical research groups have proposed the use of non-gated real-time (RT) MRI sequences [10,13]. These highly accelerated imaging techniques sacrifice spatial resolution and signal-to-noise ratio (SNR) compared to breath held, ECG gated cine cMRI (conventional cine) to produce images that are not corrupted by motion, see example in Fig. 3b. Although the resulting images allow assessment of cardiac function during exercise, through-plane motion of the heart during respiration and bodily movements during exercise lead to significant errors and variability in quantification of cardiac volumes and function [3] and complicate the assessment of wall motion abnormalities. Furthermore, due to the presence of multiple heart beats in one acquisition inter- and intra-observer variability in choice for target images for assessment of cardiac volumes are likely to add further errors, limiting the potential use of RT imaging for clinical application.

To account for respiratory motion during free-breathing cMRI, a navigator echo is typically added to cMRI sequences [15]. However, this method reduces temporal resolution of dynamic imaging, making it unsuitable for use during exercise. Several self-navigating (SG) sequences have recently been developed that account for respiratory and cardiac motion during cMRI. In SG, target motion is estimated directly from the acquired data. As a result, most SG techniques do not increase scan-time or reduce temporal resolution. SG techniques can be divided in image-based, k-space based, and model-based approaches. Image-based SG relies on registration of high quality dynamic images based on motion signals derived from lower temporal or spatial dimensional images reconstructed from the same dataset [11,12,14,17]. K-space based methods derive the respiratory signal from central k-space lines [4,5,9]. Finally, model-based approaches have been proposed for motion detection in cMRI. An example of such an approach is described by Yoon et al. [18], who use a low-rank method that separates the background of the image mathematically from the dynamic portions. Although the above described SG techniques have great potential for imaging during exercise, the proposed methods rely on complex k-space trajectories, such as radial [11,12] or golden angle radial [5,14,17] acquisition schemes, and computer intensive reconstruction frameworks. Unfortunately, such techniques are currently not widely available in a clinical cMRI setting, limiting their use for routine clinical exercise cMRI. Hansen et al. proposed a method for image-based respiratory gating at rest, based on a real-time cMRI sequence that is standardly available on commercial MRI systems [8]. However, this technique uses ECG waveforms for cardiac gating; a strategy that is not feasible for imaging during exercise as ECG signals are significantly disturbed due to bodily motion.

In this work, we develop and evaluate a semi-automatic framework for reconstruction of cardiac and respiratory gated cine cMRI (exGated cine) that allows for assessment of cardiac volumes, function and wall motion during strenuous physical exercise. In order to maximise application of our technique in clinical cMRI settings, we aimed for a method with minimal user interaction that can be flexibly applied on all imaging platforms without the need for advanced sequence programming or the use of intensive computing power. We show that our technique, based on a widely available real-time imaging sequence, is able to reconstruct gated cine images with improved image quality and lower inter-and intra-observer variability than non-gated RT imaging. Furthermore, we demonstrate that our method allows detection of a pathological cardiac response to exercise in patients with a heart disease.

2 Methods

We propose a strategy that involves (i) acquisition of highly accelerated dynamic (real-time) MRI using widely available acceleration techniques followed by (ii) image-based cardiac synchronisation, (iii) respiratory gating and (iv) motion correction and reconstruction of a 24–30 phase cardiac cine image stack. We evaluated our method in 10 healthy volunteers and 10 patients with congenital heart diseases (CHD) and exercise intolerance. Dynamic imaging datasets were acquired at moderate and high intensity, supine bicycle ergometer exercise corresponding to a heart rate (HR) of ∼100–110 beats per minute (bpm) and ∼135–150 bpm, respectively. As routinely used clinical cine cMRI (conventional cine) is not feasible during exercise, we compared exGated cine with a previously validated, non-gated real-time imaging protocol (non-gated RT) that uses manual selection of respiratory state using a dedicated cardiac analysis software package (RightVol, KU Leuven) [10]. We assessed agreement between the two methods using Pearson's correlation, assessed inter- and intra-observer variability with Bland Altman plots and tested for difference in variance between the two methods using the F-ratio. Image quality was rated using a 5-point Image Quality Score (IQS; 1 = unsuitable for diagnostic use, 5 = similar to conventional cine imaging at rest) by two blinded imaging-cardiologist. Lastly, we compared systolic function between healthy volunteers and patients with CHD during exercise using a repeated measures ANOVA with exercise intensity as the within-subject effect. Values are expressed as means ± SD. $p < .05$ was considered statistically significant. The main novelty of the proposed method lies in the clinical applicability of our semi-automatic, image-based reconstruction framework that creates respiratory and cardiac gated cine images of the heart during exercise without the need for intensive computing power or advanced cMRI pulse-sequences. The proposed framework is illustrated in Fig. 1. Our pipeline was implemented in MATLAB R2015b (MathWorks, Natick, USA) utilizing the signal processing, image processing and statistics toolboxes. This study has been approved by our regional ethics board (REC: 15/LO/522, Bloomsbury London,UK) and informed consent was obtained from all participants.

2.1 Highly Accelerated Dynamic MRI

Our method relies on high temporal resolution (∼35 ms/frame) dynamic imaging, using acceleration techniques that are currently available on all commercially available MRI scanners, without the need of advanced user settings. In this study, images were acquired on a 1.5T MRI scanner (Ingenia, Philips Medical, Best, The Netherlands). Steady-state free precession imaging was performed without cardiac gating. 80–100 consecutive frames were acquired over 14 slices with a thickness of 8 mm in a short axis orientation. Imaging parameters were: field of view, 300×260 mm (approx.); flip angle 50°; SENSE factor 3 (Cartesian k-space undersampling); partial Fourier factor 0.5, repetition time 1.8 ms; echo time 0.9 ms and reconstruction-matrix, 128×112, resulting in a reconstructed voxel size, $2.3 \times 2.3 \times 8$ ms and a frame rate of ∼35 ms. After acquisition, a region of interest around the heart (cROI) and a centre point for the LV were manually selected on an average of all images to facilitate the reconstruction process. This is the only manual step of our pipeline.

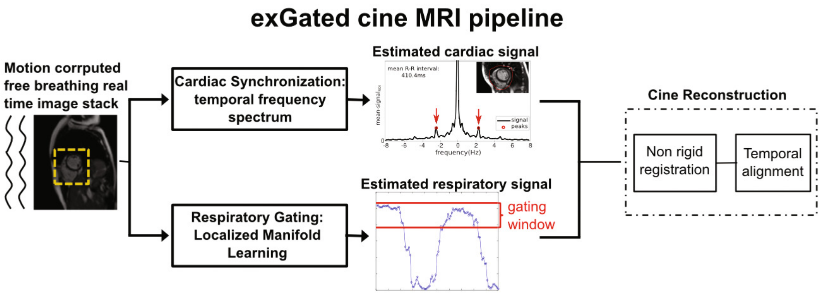

Fig. 1. Overview of the proposed framework for cardiac and respiratory gated MRI during exercise.

2.2 Cardiac Synchronization

ECG signals, routinely used for cardiac gating in cMRI, are significantly distorted during physical exercise. However, the high temporal resolution of our acquisition allows for direct estimation of the cardiac periodicity from the images, as was previously demonstrated by van Amerom *et al.* [1]. In order to obtain cardiac gating, we estimated the cardiac periodicity during exercise by transforming the images to the frequency domain and taking the spatial mean of the cROI. Before Fourier transformation the signal was interpolated to a resolution of 0.03 bpm (0.05 mHz) by zero-padding in the time domain. The local maxima in the frequency spectrum within the range of fundamental frequencies (0.8–2.8 Hz) were identified and used to calculate cardiac periodicity (see Fig. 2a). Subsequently, each frame was assigned to an associated cardiac phase bin based

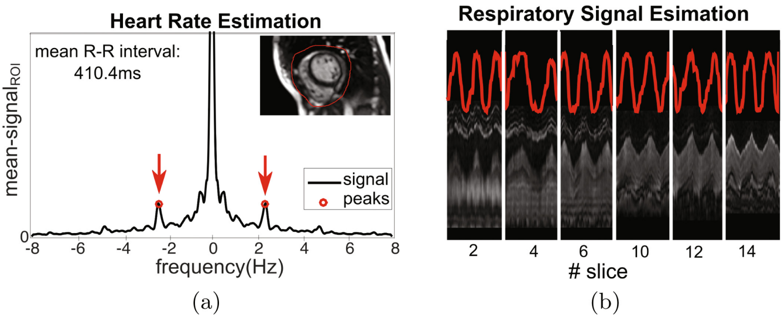

Fig. 2. (a) Range of fundamental frequencies (1.8–2.7 Hz) of the temporal frequency domain, estimated cardiac rate on the ROI appeared as the maxima (red arrows). (b) Estimated respiratory signal (red line) overlay to a spatio-temporal intensity profile through diaphragm. (Color figure online)

on the cardiac time interval. For HRs <130 bpm, the cardiac time interval was divided in 30 equally spaced cardiac phase bins, whereas for higher HRs the frames were divided over 24 cardiac phase bins. In both cases, the temporal resolution (in cardiac phases) of the cine reconstructions comply with guidelines for cine acquisitions in routine clinical cardiac MRI [6].

2.3 Respiratory Gating

In order to resolve high quality gated cine imaging of the heart, respiratory motion needs to be corrected. As respiratory excursions result in a high degree of through-plane motion of the heart, simply averaging respiratory cycle motion throughout the acquisition would lead to significant blurring of the reconstructed images. This also deviates from the current standard of end-expiratory assessment of cardiac volumes. We therefore applied Laplacian Eigenmaps, a Manifold Learning (ML) technique, in order to automatically estimate the respiratory motion in each slice in the imaging stack based on image intensity [17]. ML projects a higher dimensional manifold (e.g., an image of large dimensions) to a corresponding low dimensional representation. Previous work has shown that this technique is be able to accurately estimate a 1D representation of respiratory motion from dynamic cardiac imaging at rest [17]. As the ML estimated respiratory signal may have cardiac component due to high temporal resolution of real-time images, we filtered this signal in the frequency range of 0.1–0.5 Hz in order to retain the respiratory component. Subsequently a predefined respiratory gating window was used to select the images at end-expiration (20% of respiratory movement from maximal expiration) for further reconstruction. This gating window is equivalent to a ∼6–8 mm gating window using a respiratory navigator echo. Figure 2b shows an example of the ML estimated respiratory signal overlaid on a spatio-temporal intensity profile through diaphragm.

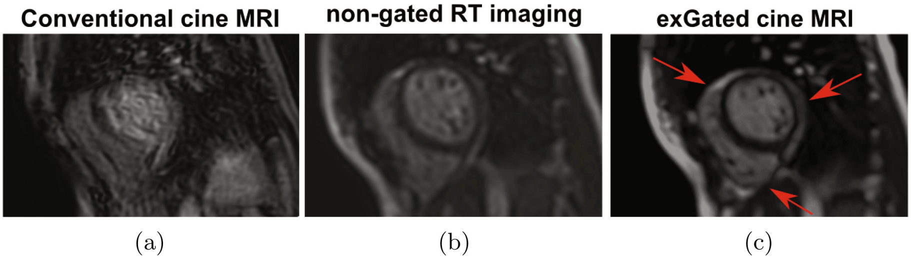

Fig. 3. Cardiac reconstructed MRI images: (a) conventional cine MRI, (b) non-gated RT MRI [10], (c) proposed approach - exGated cine MRI. Arrows denote better delineation of pericardium fat and RV wall of the proposed method.

2.4 Cine Reconstruction

After cardiac and respiratory gating, the most representative image within each cardiac phase bin was selected by computing the mean-square error between all image pairs in that bin. The image with lowest error with respect to all other images was selected as the reference image. Subsequently, a Demons non-rigid registration algorithm [16] was used to estimate the set of displacement fields that aligns each image to this reference image. All images were registered and averaged to form a unique image per bin, hereby improving SNR. In order to assure temporal alignment of the cardiac phases between all slices, we segmented the LV blood pool using an automatic segmentation algorithm based on Otsu's method that was guided by the cROI and LV centre point. The smallest segmentation of each slice was selected as the end-systolic frame. Based on this reference frame all slices were temporally aligned. Finally, a rigid body in-plane image registration was performed to register the position of the heart over time to reduce inter-frame exercise motion, facilitating the interpretation of ventricular contraction and wall motion abnormalities.

3 Experiments and Results

All datasets were successfully reconstructed to exGated cine stacks that allowed volumetric analysis. There was good agreement in ventricular stroke volume (SV) between exGated cine and non-gated RT imaging (R = 0.82). Bland Altman analysis of the two methods and their respective inter- and intra-observer agreement are shown in Figs. 4 and 5. The inter- and intra-observer variance of SV was significantly lower in exGated cine compared to RT imaging (intra-observer: $F_{(29,29)} = 2.75$, $p < .01$ and inter-observer: $F_{(29,29)} = 3.01$, $p < .01$). The IQS was $1.1 \pm .3$ for conventional cine, $3.1 \pm .6$ for non-gated RT and $3.9 \pm .5$ for exGated cine (see Fig. 6). Figure 3 shows an example of conventional cine, non-gated RT MRI and our gated cine approach, with good delineation of pericardial fat and RV-wall obtained by our proposed method. Lastly, we show that

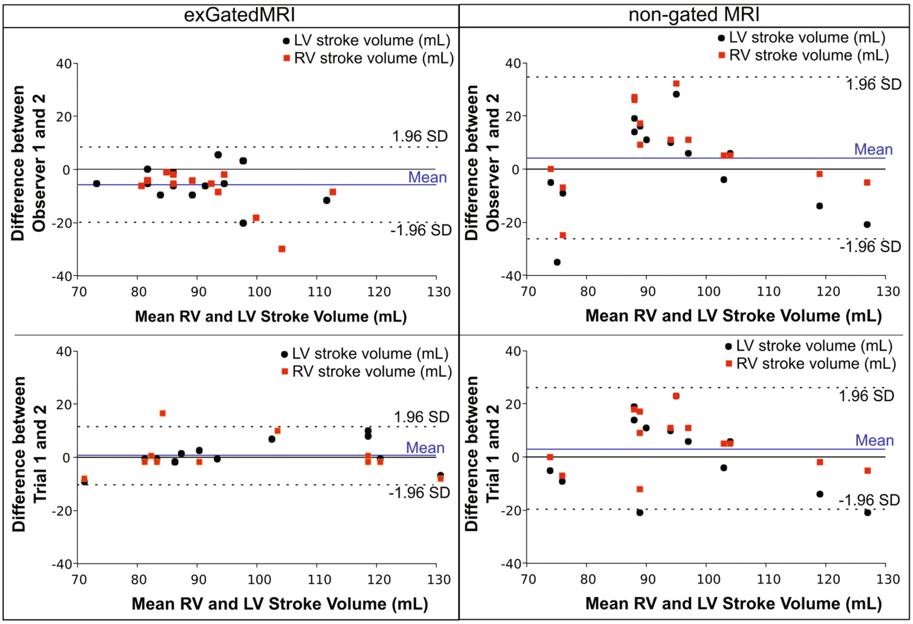

Fig. 4. Bland Altman plots of inter- and intra-observer variability of stroke volume (mL) of the two methods. Note the smaller limits of agreement and variance in exGated Cine.

the increase in LV systolic function (measured by ejection fraction) was significantly lower in patients with congenital heart disease and exercise intolerance compared to healthy volunteers ($p < .01$ for both moderate and high exercise), see Table 1.

Table 1. Ejection Fraction during exercise for patients with complex congenital heart disease (CHD) and healthy volunteers using the exGated cine MRI.

LV ejection fraction (%)	Healthy Volunteers (n = 10)	Patients with complex CHD (n = 10)
Rest	62 ± 5	51 ± 8
Moderate[a]	68 ± 4	53 ± 6
High[a]	74 ± 6	55 ± 4

[a]represents $p < .05$.

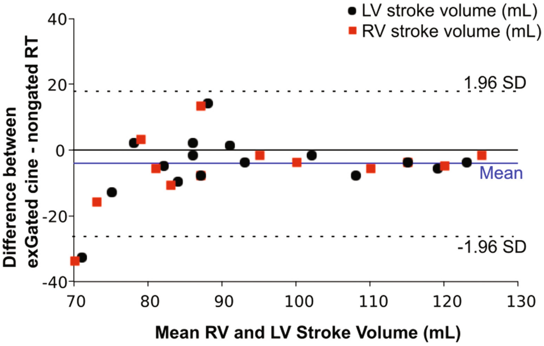

Fig. 5. Bland Altman plot of agreement in stroke volume (mL) between exGated cine and non-gated RT.

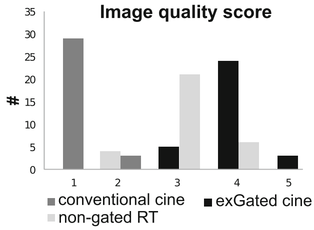

Fig. 6. Image quality score between conventional cine MRI (white bar), non-gate RT [10] (gray bar) and our proposed approach - exGated cine MRI (black bar).

4 Discussion

In this work, we present a reconstruction pipeline for cardiac and respiratory gated cine cMRI that allows for accurate assessment of cardiac function during strenuous physical exercise. Imaging of the heart during exercise has so far been restricted due to bodily motion and cardiac gating issues. However, its widely recognized potential for disease evaluation [2] appeals for exploration of techniques to enable exercise cMRI. No satisfying technique has yet been developed that allows widespread clinical implementation of exercise cMRI. RT imaging strategies suffer from significant errors in quantitative assessment due to respiratory motion [3]. Whereas SG strategies, recently developed and applied in MRI at rest [4,5,7,11,14,17], require custom-build cMRI pulse sequences and computationally expensive reconstruction schemes that are currently not available in most clinical cMRI environments.

We developed a method for exercise cMRI that can be directly applied in clinical practice. Our proposed reconstruction framework starts with the acquisition of a stack of highly accelerated dynamic images. This type of dynamic cMRI sequences is currently available on all commercial MRI scanners. Our proposed reconstruction framework starts with the acquisition of a stack of highly accelerated dynamic images. This type of dynamic cMRI sequences is currently available on all commercial MRI scanners. We exploit the temporal resolution of the acquired images for image-based estimation of cardiac and respiratory motion. By using image-based techniques, we avoid the use of raw image data and complex reconstruction techniques. In order to keep computational expenses low, we utilize dimensional reduction in our motion estimation techniques. As a result, our framework is able to reconstruct a cine stack of the heart in a clinically acceptable total reconstruction time of ∼30–40 min using a standard laptop computer.

We used ML to estimate motion from the acquired stack of dynamic images. This method has previously been used in combination with dynamic imaging and shown to be both robust and fast [17]. We found that respiratory motion was accurately estimated with the ML using the entire image as input (see Fig. 2b). ML did also detect a cardiac signal. However, the cardiac periodicity estimation based on this signal proved to be not precise enough for cardiac gating, due to significant shifts in image intensities as a result of through-plane motion of the heart and surrounding fat. Estimation in the temporal frequency domain proved more accurate. However, we needed to introduce a cROI in order to avoid the detection of exercise motion.

We implemented our proposed reconstruction pipeline in our clinical cMRI facility and showed that the output of our reconstruction pipeline, exGated cine, is in acceptable agreement with non-gated RT imaging for SV. There is some variability in quantification of SV noted between the two methods. However, inter- and intra-observer variability of exGated cine was superior compared to non-gated RT imaging. These results most likely reflect the improved accuracy of exGated cine, as quantification errors introduced by respiratory motion in non-gated RT imaging are eliminated [3]. This improved repeatability in quantification of SV is an important gain of our technique, as it facilitates implementation of exercise cMRI in a clinical setting.

Finally, we demonstrated that our method was able to detect a clear pathophysiologic response to exercise in patients with CHD, expressed by the significantly lower increase in systolic function compared to healthy volunteers. This highlights the potential advantages of exercise cMRI for clinical cardiology. Our work is a preliminary step in the application of image processing techniques in the emerging field of exercise cMRI. We aim to improve our method further by implementing automatic segmentation techniques for detection and segmentation of the LV bloodpool. Some recently proposed self-gated cMRI sequences could have important potential for imaging during exercise. Unfortunately, translation of such techniques to clinical settings remains challenging. We hope that our work is an encouragement for development and implementation of these techniques for clinical exercise cMRI.

References

1. van Amerom, J., Lloyd, D., Price, A., Kuklisova Murgasova, M., Aljabar, P., Malik, S., Lohezic, M., Rutherford, M., Pushparajah, K., Razavi, R., et al.: Fetal cardiac cine imaging using highly accelerated dynamic MRI with retrospective motion correction and outlier rejection. Magn. Reson. Med. (2017)
2. Cahalin, L., Chase, P., Arena, R., Myers, J., Bensimhon, D., Peberdy, M., Ashley, E., West, E., Forman, D., Pinkstaff, S., et al.: A meta-analysis of the prognostic significance of cardiopulmonary exercise testing in patients with heart failure. Heart Fail. Rev. **18**(1), 79–94 (2013)

3. Claessen, G., Claus, P., Delcroix, M., Bogaert, J., La Gerche, A., Heidbuchel, H.: Interaction between respiration and right versus left ventricular volumes at rest and during exercise: a real-time cardiac magnetic resonance study. Am. J. Physiol. Heart Circ. Physiol. **306**(6), H816–H824 (2014)
4. Crowe, M., Larson, A., Zhang, Q., Carr, J., White, R., Li, D., Simonetti, O.: Automated rectilinear self-gated cardiac cine imaging. Magn. Reson. Med. **52**(4), 782–788 (2004)
5. Feng, L., Axel, L., Chandarana, H., Block, K.T., Sodickson, D.K., Otazo, R.: XD-GRASP: golden-angle radial MRI with reconstruction of extra motion-state dimensions using compressed sensing. Magn. Reson. Med. **75**(2), 775–788 (2016)
6. Fratz, S., Chung, T., Greil, G., Samyn, M., Taylor, A., Buechel, E., Yoo, S.J., Powell, A.: Guidelines and protocols for cardiovascular magnetic resonance in children and adults with congenital heart disease: SCMR expert consensus group on congenital heart disease. J. Cardiovasc. Magn. Reson. **15**(1), 51 (2013)
7. Han, F., Zhou, Z., Han, E., Gao, Y., Nguyen, K.L., Finn, J., Hu, P.: Self-gated 4D multiphase, steady-state imaging with contrast enhancement (MUSIC) using rotating cartesian K-space (ROCK): validation in children with congenital heart disease. Magn. Reson. Med. (2016)
8. Hansen, M., Sørensen, T., Arai, A., Kellman, P.: Retrospective reconstruction of high temporal resolution cine images from real-time MRI using iterative motion correction. Magn. Reson. Med. **68**(3), 741–750 (2012)
9. Kim, W., Mun, C., Kim, D., Cho, Z.: Extraction of cardiac and respiratory motion cycles by use of projection data and its applications to nmr imaging. Magn. Reson. Med. **13**(1), 25–37 (1990)
10. La Gerche, A., Claessen, G., Van de Bruaene, A., Pattyn, N., Van Cleemput, J., Gewillig, M., Bogaert, J., Dymarkowski, S., Claus, P., Heidbuchel, H.: Cardiac MRI: a new gold standard for ventricular volume quantification during high-intensity exercise. Circ. Cardiovasc. Imaging **6**(2), 329–338 (2013)
11. Larson, A., White, R., Laub, G., McVeigh, E., Li, D., Simonetti, O.: Self-gated cardiac cine MRI. Magn. Reson. Med. **51**(1), 93–102 (2004)
12. Liu, C., Bammer, R., Kim, D.H., Moseley, M.: Self-navigated interleaved spiral (SNAILS): application to high-resolution diffusion tensor imaging. Magn. Reson. Med. **52**(6), 1388–1396 (2004)
13. Lurz, P., Muthurangu, V., Schievano, S., Nordmeyer, J., Bonhoeffer, P., Taylor, A., Hansen, M.: Feasibility and reproducibility of biventricular volumetric assessment of cardiac function during exercise using real-time radial k-t SENSE magnetic resonance imaging. J. Magn. Reson. Imaging **29**(5), 1062–1070 (2009)
14. Paul, J., Divkovic, E., Wundrak, S., Bernhardt, P., Rottbauer, W., Neumann, H., Rasche, V.: High-resolution respiratory self-gated golden angle cardiac MRI: comparison of self-gating methods in combination with k-t SPARSE SENSE. Magn. Reson. Med. **73**(1), 292–298 (2015)
15. Peters, D.C., Nezafat, R., Eggers, H., Stehning, C., Manning, W.J.: 2D free-breathing dual navigator-gated cardiac function validated against the 2D breath-hold acquisition. J. Magn. Reson. Imaging **28**(3), 773–777 (2008)
16. Thirion, J.P.: Image matching as a diffusion process: an analogy with Maxwell's demons. Med. Image Anal. **2**(3), 243–260 (1998)
17. Usman, M., Atkinson, D., Kolbitsch, C., Schaeffter, T., Prieto, C.: Manifold learning based ECG-free free-breathing cardiac CINE MRI. J. Magn. Reson. Imaging **41**(6), 1521–1527 (2015)
18. Yoon, H., Kim, K., Kim, D., Bresler, Y., Ye, J.: Motion adaptive patch-based low-rank approach for compressed sensing cardiac cine MRI. IEEE Trans. Med. Imaging **33**(11), 2069–2085 (2014)